

COMPARISON OF FEM AND FVM FOR THE NUMERICAL SIMULATION OF FORGING PROCESS

JAN RIHACEK, EVA PETERKOVA, MICHAELA CISAROVA, JAROSLAV KUBICEK

Brno University of Technology, Faculty of Mechanical Engineering, Institute of Manufacturing Technology, Brno, Czech Republic

DOI : 10.17973/MMSJ.2020_03_2019151

e-mail: rihacek.j@fme.vutbr.cz

The paper deals with a study and a comparison of numerical simulations of a bearing ring production using various numerical methods for solution. The bearing ring is produced by forging technology in three operations. The study is focused on the first two operations, i.e. upsetting and forging of the final shape of the part. Numerical simulation of the mentioned manufacturing process is performed in Simufact Forming software, which allows the use of finite element method as well as finite volume method. In this case, 2D and 3D FE solution and also FV calculation using first and higher order solver are compared, followed by comparison with real production.

KEYWORDS

finite element method, finite volume method, forging, bearing ring, Simufact Forming

1 INTRODUCTION

Due to the growing pressure on innovation and an available theoretical knowledge, a rapid prediction of manufacturing results and an optimization of newly designed production processes is increasingly needed, even in the forging technology. These problems in complexity can be solved by using numerical analysis within the area of computer-aided engineering. In the present time, there are a number of numerical methods that can be used for calculations in the field of forming technologies. These methods differ from one another based on conversion of the physical problem descriptions into a mathematical model. For this reason, their use across technical practice also differs. In the field of the forging analysis, the most widely used methods are the well known finite element method (FEM) and also finite volume method (FVM).

In principle, FEM is based on the discretization of the continuous continuum into a finite number of elements, see Fig. 1a. The investigated parameters are then determined in individual nodes of these elements located on tops of each element and distributed throughout them using its shape functions. In the case of the formed part deformation, the finite element mesh deforms with it because it is firmly bound to it. It is so called Lagrangian approach. The problem of using the finite element method for forming processes is mainly the excessive deformation of the finite element mesh during large deformations of the formed parts. Due to the large distortion of FEM elements, there are inaccuracies in the calculation and it is necessary to perform a remeshing, i.e. replacement of distorted mesh with a new one during the calculation, which extends the calculation time, among other things. It is important to note, that the computation accuracy of FEM also depends on the FEM element type used. [Valberg 2010]

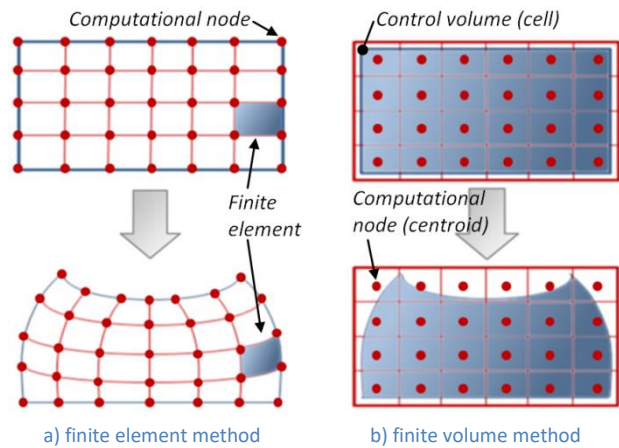


Figure 1. Basic schemes of FE and FV methods [Buijk 2008]

On the other hand, FVM uses a set of control volumes for discretization of the solved problem, wherein the volume of the formed part substantially flows from one control volume to another using so called Euler solver, as it is shown in Fig. 1b. The actual calculation is then realized using computational nodes in the middle of each of the control volumes (cells). The values of velocity components and scalar quantities are thus calculated in the geometric centers of the control volumes. The values at the volume boundaries being obtained by an interpolation. This is also one of the main drawbacks of this method, since it is highly dependent on how the interpolation is performed. It is possible to note that the material in the control volumes can also interact with Lagrangian structures during the Euler calculation, i.e. it can act by forces on the mentioned structure causing deformations. On the other hand, Lagrangian structures are able to provide a barrier to the Eulerian material. Because of the impossibility of coordinate transformations during the calculation, FVM uses so called coupling surfaces to define a multifaceted object in the calculation, i.e. the FV solver is applied to the 3D object that consists of that part of the control volume (cell) that is inside the mentioned coupling surface, see Fig. 2. [Van Der Veen 2005]

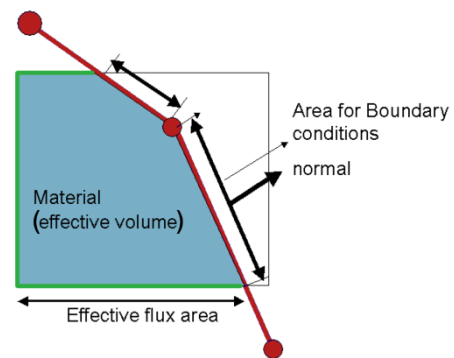


Figure 2. Boundary of FVM control volume [Van Der Veen 2005]

Fig. 2 represents Boundary of FVM control volume in 2D space, where a square constitutes the control volume which is intersected by the coupling surface. The part of this square that is inside the coupling surface is called the effective volume and it can contain mass. The boundary of the effective volume is composed of two surfaces types: Cell boundaries connecting adjacent control volumes (green line in the figure) and parts of the coupling surface inside the control volume, i.e. so called polyhedron packets - polpacks (red line in the figure). During the computation, it is necessary to compute these polyhedron packets for the given geometry boundary of the formed part to calculate the contribution from one control volume to another over the effective flux area. [Plugge 2005]

2 SOLVED PROBLEMATICS

The solved part is a simple bearing ring, which is produced by using forging technology in three operations. Firstly, a blank is cut from a 32 mm diameter rod and it is heated to the desired forging temperature. In this case, the optimum forging temperature is approx. 1 150 °C.

In the first forming operation, the blank is upsetted, which is followed by forging into the final shape. In the last operation an arised web is trimmed. All forging operations are performed on Hatebur AKS 63 machine. The shape of the part and its main dimensions during the forging process, except trimming, are shown in Fig. 3.

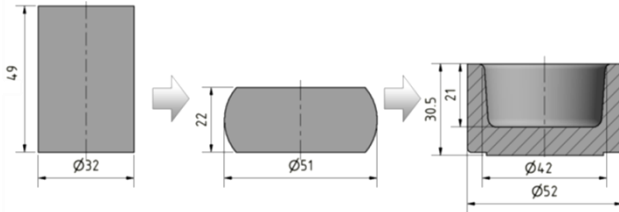


Figure 3. The shape and main dimensions of the produced profile

In a serial production, the bearing ring is made of 100Cr6 (1.3505) steel. Mentioned material is mainly intended for rolling contact and other high fatigue applications. In a practise, it is used for components that require high tensile strength and high hardness, which is also the case of the manufactured part. Main mechanical properties and chemical composition of 100Cr6 steel are summarized in Tab. 1 and Tab. 2.

Minimal upper yield stress	R_{eH}	[MPa]	352–373
Ultimate strength	R_m	[MPa]	561–567
Minimal ductility	A_t	[%]	29.5–31.3
Relative contraction	Z	[%]	66.7–66.9

Table 1. Mechanical properties of S355J2 steel

%C	%Mn	%Si	%P	%S	
0.220	1.250	0.390	0.019	0.010	
%Cu	%Cr	%Ni	%Al	%Mo	%V
0.03	0.08	0.03	0.028	0.014	0.003

Table 2. Chemical composition of S355J2 steel

3 NUMERICAL SIMULATION

For the forging simulation of the above mentioned issue, the Simufact Forming software version 15 was used to verify the manufacturability. The software uses customized versions of the finite element solver MSC Marc and MSC Dytran as the finite volume solver. [Simufact 2018]

Verification of the above mentioned manufacturing design was performed for several solution variants that use both the finite element method and also the finite volume method. In the Simufact forming software, there are several possibilities available, namely FE solver for 2D axisymmetric and full 3D geometry and also FV solver for 3D geometry using 1st order or higher order solution algorithm. It should be noted, that it was necessary to create a slightly different geometrical model that corresponds to every single calculation for each solution variant. However, the geometrical model has always been in principle based on CAD models of tools in the first and second operations, as it is shown in Fig. 4. [Sigmund 2019], [Simufact 2018]

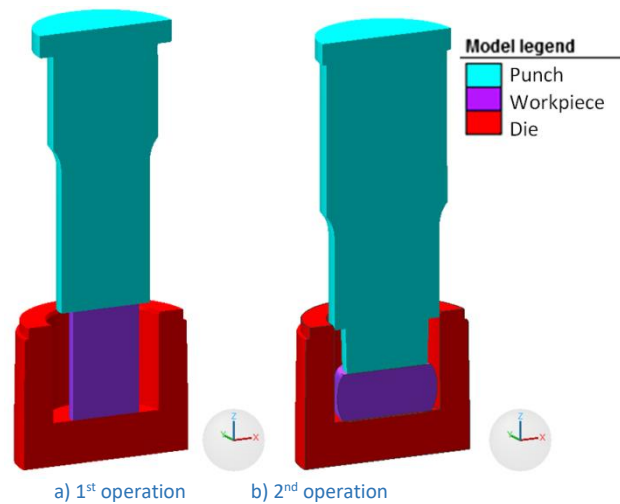


Figure 4. Geometrical model for the numerical simulation

In the next, Fig. 5 shows the differences in discretization, i.e. a creation of the FE mesh and the FV mesh for 3D simulation.



Figure 5. Example of computational mesh / volume for 2nd operation

Ideally rigid tools were considered, whose velocity was set according to crank mechanism of Hatebur AKS 63 machine. For definition of the blank material model, the material database of Simufact Forming software was used. Plastic properties of the material were defined by GMT model, where the flow stress curves are defined by following equation, which includes the influence of temperature and strain rate according to:

$$\sigma = C_1 \cdot e^{(C_2 \cdot T)} \cdot \varphi^{(n_1 \cdot T + n_2)} \cdot e^{\left(\frac{l_1 \cdot T + m_2}{\varphi}\right)} \cdot \dot{\varphi}^{(m_1 \cdot T + m_2)} \quad (1)$$

where σ is the flow stress [MPa], φ is the effective plastic strain [-], $\dot{\varphi}$ is the strain rate [s^{-1}], C_1 , C_2 , n_1 , n_2 , l_1 , l_2 , m_1 and m_2 are material parameters [-]. [Simufact 2018]

The flow stress curves of 100Cr6 steel for different values of temperature and strain rate are shown in Fig. 6.

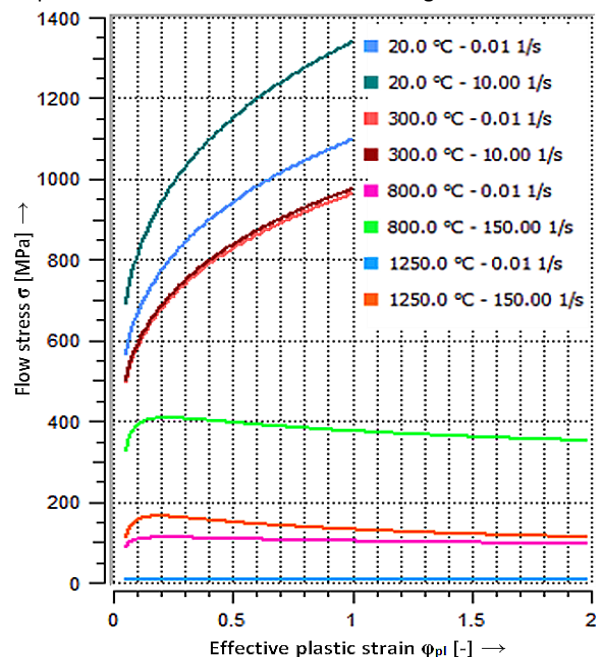


Figure 6. Flow stress of 100Cr6 steel

Temperature of the initial workpiece was set to 1 150 °C and ambient temperature was considered as 50 °C. Thermal properties were also determined based on data from the Simufact Forming database with considered thermal exchange with the workpiece as $\alpha = 20 \text{ W}\cdot\text{m}^{-2}\cdot\text{K}^{-1}$. In the next, friction properties were set using the combined model with Coulomb coefficient 0.2 and shear stress friction factor of 0.4. In order to make the comparison of the methods as representative as possible, the same size of computational mesh elements was used for both FE and FV solutions, of course with maintaining the same settings for all boundary parameters. Initial meshing strategy used a quadrilateral element for 2D simulation. Due to convergence of the calculation, it was necessary to use tetrahedral elements for FEM 3D simulation and triangle elements for polpacks of FV solution. The initial element size was set to 1.5 mm. In the case of remeshing of FE mesh or FV polpacks, 1 mm was used for critical plastic strain change of 0.3.

4 RESULTS AND DISCUSSION

After the calculation, it is possible in post-processing to focus on simulation results of 1st and 2nd forging operation. Firstly, the computation time was investigated. The results are summarized in Tab. 3 and Tab. 4.

Method	Initial number of elements	CPU time [s]
FEM - 2D	320	51.98
FEM - 3D	26 180	36 601.78
FVM - 1 st order	polpacks: 6 032 control volumes: 15 972	6 157.86
FVM - higher order	polpacks: 6 032 control volumes: 15 972	8 490.96

Table 3. Required CPU times for calculation of 1st operation

Method	Initial number of elements	CPU time [s]
FEM - 2D	1 000	243.11
FEM - 3D	104 931	94 895.47
FVM - 1 st order	polpacks: 13 040 control volumes: 16 335	6 155.65
FVM - higher order	polpacks: 21 147 control volumes: 16 335	7 958.45

Table 4. Required CPU times for calculation of 2nd operation

In the next, Fig. 7 to Fig. 10 show the prediction of effective plastic strain. As it is evident from results, the distribution of the effective plastic strain is quite different for various computational methods. The variance in maximum observed values is 0.48 for 1st operation and even 1.53 for 2nd operation. It is possible to note, that results, which were determined by FVM, show generally lower strain values as well as higher diffusion of calculated values compared to FEM.

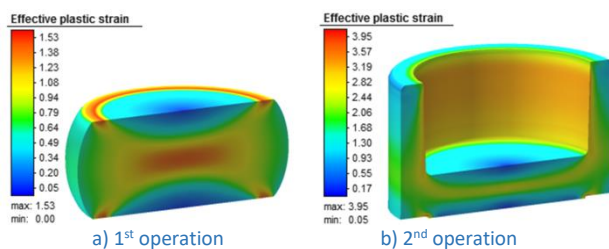


Figure 7. Effective plastic strain by using FEM 2D simulation

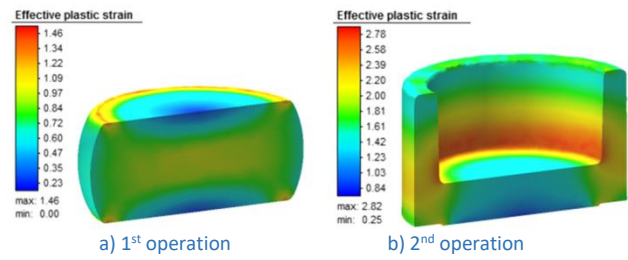


Figure 8. Effective plastic strain by using FEM 3D simulation

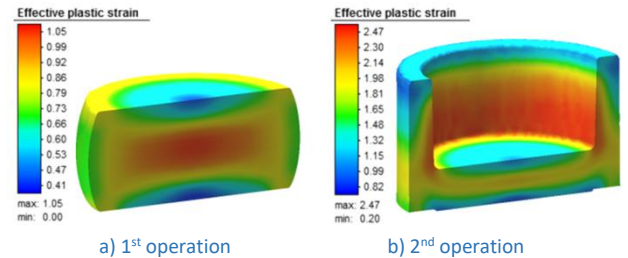


Figure 9. Effective plastic strain by using FV - 1st order 3D simulation

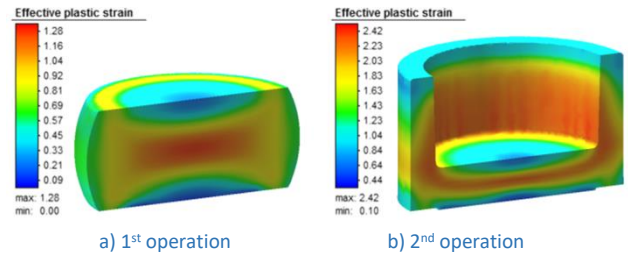


Figure 10. Effective plastic strain by using FV - higher order 3D simulation

Another way to compare these approaches to the solution is the analysis of the material flow. In this case, a deformation of the grid pattern simulating material fibers can be observed using so called flowlines. In Fig. 11, flow lines deformation in 1st operation is shown.

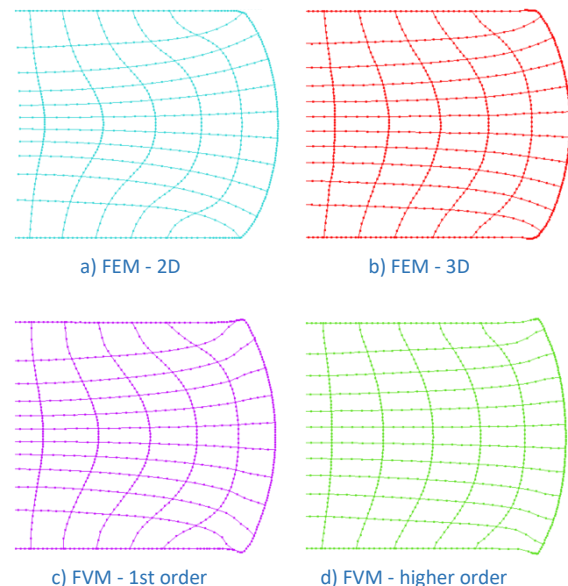


Figure 11. Deformation of the grid pattern after 1st operation

Obviously, for simpler shape changes, such as upsetting, there are no major differences between the predicted material flow. But even in this case is obvious, that FVM shows worse binding of flowlines to the basic geometry of the deformed workpiece. As a result, deviation of flowlines geometry on the upper and lower edges of the workpiece can be observed, which can be also evident in the overall comparison in Fig. 12.

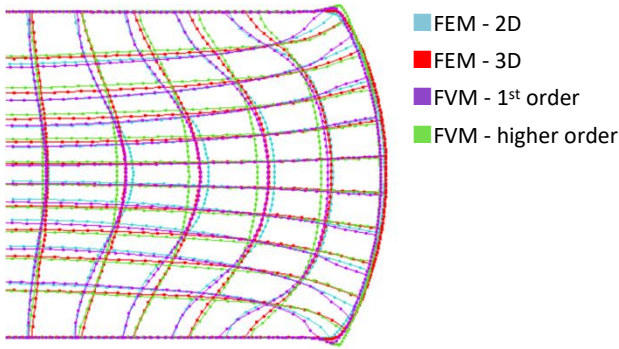


Figure 12. Deformation of the grid pattern after 1st operation for all computational methods

Larger deviations in the calculated material flow are achieved in 2nd operation, see Fig. 13. While FEM shows real results and only the transition at the bottom of the workpiece, which is too small to flowlines to capture, seems problematic, FVM is not able to bind the flowlines grid to the workpiece without problems. This is especially true of the part contour. Therefore, it makes an unreasonable warp of the grid that extends beyond the workpiece into the tool.

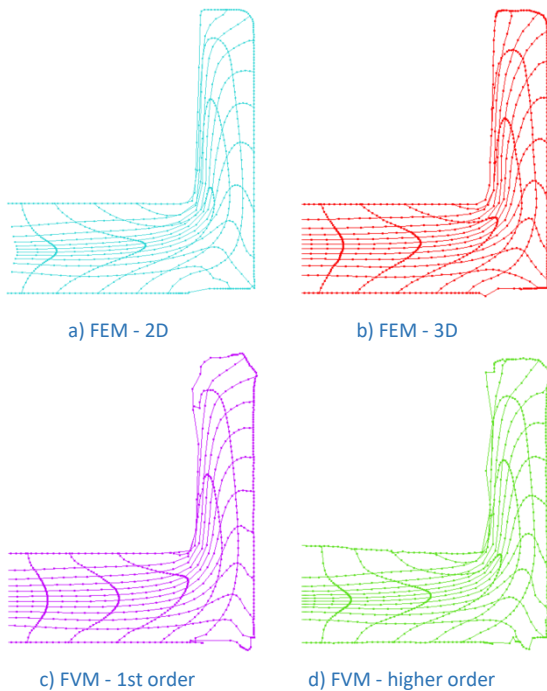


Figure 13. Deformation of the grid pattern after 2nd operation

For more accurate comparison with real manufacturing process, a specimen etching was also performed to make the material fibres visible, as it is shown in Fig. 14.



Figure 14. Deformation of material fibres

This fact also can be observed in the comparison in Fig. 15. On the other hand, it should be mentioned that FV solution using higher order algorithm quite accurately follows the shape of fibres inside the analyzed part. Similar results are reached by FE analysis for 2D axisymmetric solution.

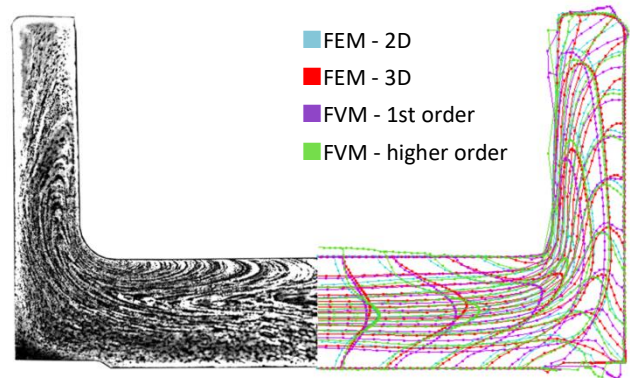


Figure 15. Comparison of material fibers deformation after 2nd operation

Of course, the mentioned differences also have an influence on the forming force determination. For 1st and 2nd operation. The curves of forging forces in dependence to the tool stroke are shown in Fig. 16 and Fig. 17.

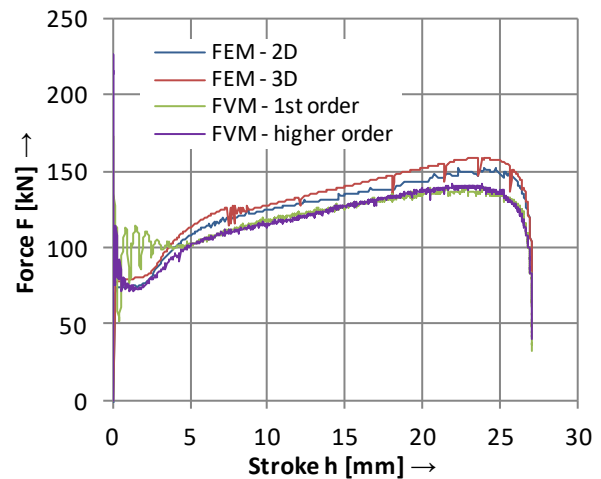


Figure 16. Forging force – tool stroke diagram for 1st operation

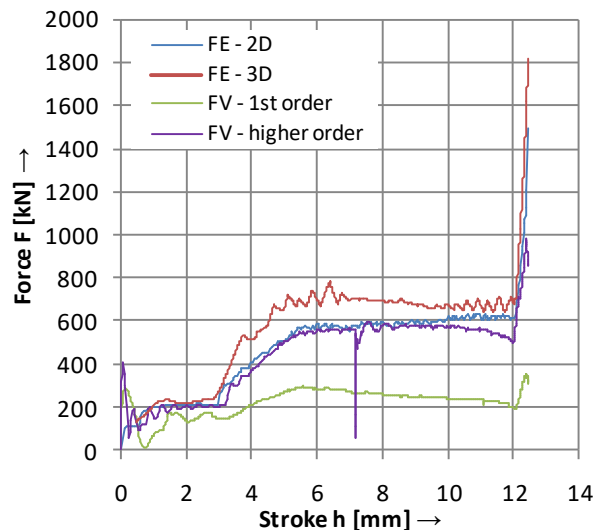


Figure 17. Forging force – tool stroke diagram for 2nd operation

The simulation results can be compared with measured data from the Hatebur AKS 63 machine. Unfortunately, machine sensors do not allow plotting of the whole curve (force – stroke diagram), but only the maximum value.

Moreover, determined value is subject to a possible error caused by the transmission of the force effect through the machine mechanism. For this case, it is rather an estimation of the real forming force. However, after comparison of the experimentally determined value with the simulation results, a comparison can be obtained, see tabulated data in Tab. 5 and Tab. 6.

Method	Maximal force [kN]	Measured maximal force [kN]	Difference [%]
FEM - 2D	152.66	150.43	1.46
FEM - 3D	163.58		8.04
FVM - 1 st	139.78		7.08
FVM - higher order	141.16		6.16

Table 5. The comparison of maximal forming forces in 1st operation

Method	Maximal force [kN]	Measured maximal force [kN]	Difference [%]
FEM - 2D	1 492.29	1 378.23	8.99
FEM - 3D	2 063.03		33.19
FVM - 1 st	313.696		77.23
FVM - higher order	979.28		28.94

Table 6. The comparison of maximal forming forces in 2nd operation

The maximal force comparison shows that the closest to the real results is a solution using FEM 2D axisymmetric and then FVM higher order computation.

5 CONCLUSIONS

The study of the manufacturability, the material flow and the force load, was performed for the bearing ring part, which is made of 100Cr6 steel on Hatebur AKS 63 machine.

In order to verify the accuracy of numerical calculation possibilities, finite element and also finite volume simulations of two main operations were performed by using Simufact Forming software. Priority was to compare these methods of calculation as far as possible the same size setting elements, etc. In post-processing, simulations results were compared with each other and, in the case of material flow and the maximum forming force, simulations results were also compared with the real produced part. In this case, four variants of the numerical solution were tested, i.e. FEM calculation for 2D axisymmetric and full 3D geometry and FVM using 1st order and higher order solution algorithm.

The results indicate possible applicability of both FEM and FVM for solving the mentioned problem. Thus, we can conclude not only from a consistent or similar prediction of the grid pattern, but also from force-stroke diagrams. In this context, it should be noted that force comparison with reality was based on only one measured value (maximum forming force) for each case. Therefore, this is only an estimate. Still, there was an effort to compare force-stroke diagrams, even with only a single value, so it needs to be taken with some margin. In any case, the comparison is problematic in unknownness of the whole force-stroke diagram, as it is evident in particular in the second operation. However, it certainly allows comparisons of mentioned methods each other.

It should also be noted that the application of FVM is still problematic in some areas. In particular, it is the analysis of material flow using the deformation of the grid pattern which, in

the case of greater deformation, makes it difficult to follow the contour of the formed part. From this point of view, FVM seems to be inaccurate for monitoring the material flow near the surface of the analysed components, e.g. the formation of relocations monitoring. However, the indisputable advantage of FVM is a lower calculation time, compared to 3D FEM solutions, and a relatively accurate determination of the forging force when using the higher-order solver, in comparison with FEM – 3D.

ACKNOWLEDGMENTS

The contribution was supported by specific research project no. VAV13313 with the support of cooperation between Brno University of Technology, Faculty of Mechanical Engineering and Šroubárna Kyjov company.

REFERENCES

- [Buijk 2008] Buijk, A. J. Finite Volume and Finite Element Integration in Simufact Forming. Simufact-Americas LLC, 2008, United States [online]. 12. 2. 2015 [6. 10. 2019]. Available from <https://www.mssoftware.com/sites/default/files/2008.1_Finite_Volume_and_Finite_Element_Integration_in_SimufactForming.pdf>
- [Plugge 2005] Plugge, E. Integrating LSTC and MSC.Software Technology for Explicit Dynamics and Fluid-Structure Interaction. In: 5th European LS-Dyna Conference, Birmingham, 25-26 May, 2005. Solihull: The International Convention Centre, pp 1-14
- [Sigmund 2019] Sigmund, M. Plasma overlay welding of cobalt alloy. MM Science Journal, October 2019, Vol. 2019 No. 3, pp 2982-2986. ISSN 1803-1269
- [Simufact 2018] Simufact Engineering GmbH. Simufact Forming User's Manual: Version 15.0. Hamburg: MSC Software, 2018
- [Valberg 2010] Valberg, H. S. Applied Metal Forming including FEM Analysis. Trondheim: Norwegian University of Science and Technology, 2010. ISBN 978-05-21518-23-9
- [Van Der Veen 2005] Van Der Veen, W. A. Crushing Simulation of a Partially Filled Fuel Tank Beyond Failure. In: SAE 2005 World Congress & Exhibition, United States, 2005, pp 1-12, ISSN: 0148-7191

CONTACTS

Ing. Jan Řiháček, Ph.D.
Brno University of Technology, Faculty of Mechanical Engineering, Institute of Manufacturing Technology, Department of Metal Forming
Technická 2896/2, Brno, 616 69, Czech Republic
e-mail: rihacek.j@fme.vutbr.cz

Ing. Eva Peterková, Ph.D.
Brno University of Technology, Faculty of Mechanical Engineering, Institute of Manufacturing Technology, Department of Metal Forming
Technická 2896/2, Brno, 616 69, Czech Republic
e-mail: peterkova@fme.vutbr.cz

Ing. Michela Císařová, Ph.D.
Brno University of Technology, Faculty of Mechanical Engineering, Institute of Manufacturing Technology, Department of Metal Forming
Technická 2896/2, Brno, 616 69, Czech Republic

e-mail: cisarova@fme.vutbr.cz

Ing. Jaroslav Kubicek
Brno University of Technology, Faculty of Mechanical
Engineering, Institute of Manufacturing Technology,
Department of Welding Technology and Surface Treatment
Technická 2896/2, Brno, 616 69, Czech Republic
e-mail: kubicek@fme.vutbr.cz